https://doi.org/10.5194/egusphere-2025-4047
Preprint. Discussion started: 19 September 2025

Role of phosphorus concentration and the nitrogen to phosphate ratio in the synergistic stimulation of alkaline phosphatase activity in Laizhou Bay, China, coastal waters

Yanqun Yang[a, b, c], Xiaomeng Duan[a, b], Shengkang Liang[a, b *], Mingzheng Zhang [a, b, d], Shanshan Li [a, b], Hongguan Li [a, b], Guoling Zhang[a, b], Haoyang Ma[a, b], Xiurong Han[a, b], Xiulin Wang[a, b]

[a] Key Laboratory of Marine Chemistry Theory and Technology, Ministry of Education / Innovation Center for Ocean Carbon Neutrality, Ocean University of China, Qingdao 266100, China

[b] College of Chemistry and Chemical Engineering, Ocean University of China, Qingdao 266100, China

[c]National Marine Environmental Monitoring Center, State Oceanic Administration, Dalian 116023, China

[d]Marine Science Research Institute of Shandong Province

Correspondence: Shengkang Liang (liangsk@ouc.edu.cn)

Abstract

In coastal ecosystems, microbial alkaline phosphatase (AP) production is primarily induced by low phosphate (PO_4-P) availability but is additionally regulated by the dissolved inorganic nitrogen to phosphate (DIN:PO_4-P) ratio and seasonal

https://doi.org/10.5194/egusphere-2025-4047
Preprint. Discussion started: 19 September 2025

temperature variation. However, the dominant driver of APA surges and potential synergistic effects among these factors remain unclear. Through integrated seasonal field surveys and an enclosure experiments in Laizhou Bay, China, we demonstrate that PO_4-P seawater concentration serves as the primary control for APA induction, with a consistent threshold of 0.05 $\mu mol \cdot L^{-1}$. Below this threshold, APA exhibits a ssignificant positive correlation with the DIN:PO_4-P ratio in both the field and an enclosure experiment under P limitation (combined analysis of field and experimental data, $p < 0.01$; n=36). Notably, phytoplankton-dominated APA is evidenced in autumn. Genetic analysis confirms that AP-related gene expression increases only when PO_4-P falls below the identified threshold. These findings refine the conceptual framework for AP regulation in coastal ecosystems, highlighting the hierarchical control of phosphorus limitation over stoichiometric effects.

Keywords: Alkaline phosphatase; phosphorus limitation; phosphate concentration threshold; norganic nitrogen to phosphorus ratio; Laizhou Bay

1. Introduction

With the intensification of nitrogen (N) emissions and the control of phosphorus (P) emissions, P limitation has become widespread in global coastal waters (Zhang et al., 2024; Maavara et al., 2020; Liang et al., 2023) and has triggered adverse ecological consequences, including exacerbated eutrophication and shifts in phytoplankton community structure (Xin et al., 2019; Peñuelas and Sardans, 2022;). To cope with P limitation, microorganisms have evolved a range of strategies,

https://doi.org/10.5194/egusphere-2025-4047
Preprint. Discussion started: 19 September 2025

including an increase in inorganic phosphate transporters, induction of hydrolases for scavenging organophosphates (OP), and a reduction in P demand by replacing phospholipids with sulfur- or N-containing lipids (Van et al., 2006; Karl, 2014; Lin et al., 2016). Among these strategies, the extracellular enzymatic hydrolysis of dissolved organic phosphorus (DOP) to bioavailable inorganic P represents a critical pathway for microbial communities to overcome P limitation in coastal waters (Zhang et al., 2017; Jin et al., 2024). Understanding OP utilization mechanisms is essential to allow prediction and management ecological responses to increasing P stress in coastal ecosystems.

Alkaline phosphatase (AP) is regarded as the most common extracellular enzyme for the utilization of dissolved organophosphates (DOP) (Yamaguchi et al., 2016; Zhang et al., 2018; Jin et al., 2024). In general, alkaline phosphatase activity (APA) is induced under P-restricted conditions and inhibited at high phosphate (PO_4-P) concentrations (Dyhrman and Ruttenberg, 2006; Zhang et al., 2018). Nausch et al. (1998) found that APA increased significantly when OP concentrations were < 0.2 $\mu mol \cdot L^{-1}$. Since then, the PO_4-P threshold for the APA surge in coastal waters has been reported to range from 0.01 to 0.5 $\mu mol \cdot L^{-1}$ in various seas (Jin et al., 2024). Both temperature, microbial species dominance, trace metal concentrations, macronutrient levels and their ratio may affect APA levels and the PO_4-P threshold (Dyhrman and Ruttenberg, 2006; Mahaffey et al., 2014; Browning et al., 2017; Zhang et al., 2018; Ivancic et al., 2021; Jin et al., 2024). Temperature has also been shown to greatly influence APA via both direct effects on enzyme kinetics and indirect effects

https://doi.org/10.5194/egusphere-2025-4047
Preprint. Discussion started: 19 September 2025

on the composition of the microbial community (Toseland et al., 2013; Thomas et al., 2017). Under conditions of nitrogen (N) excess and P limitation, a high DIN:PO_4-P ratio has been confirmed to be positively correlated with APA (Bogé et al., 2017; Jin et al., 2024). Freshwater nutrient inputs can also enhance APA (Kang et al., 2019; Ivancic et al., 2021). Trace metals (Zn, Ca, etc.) affect APA because they are core enzymatic structural components, but trace metals are unlikely limit APA in offshore waters (Jin et al., 2024). The complexity of the variables influencing APA likely contributes to the lack of consensus on the conditions for its induction in coastal waters, and the interactive effects of these factors are poorly understood. Moreover, there is currently controversial research evidence as to whether there is a PO_4-P threshold concentration for APA surges to occur. Qin et al., (2021) found that APA values were very high in PO_4-rich environments during the pre-algal bloom of the dinoflagellate *Prorocentrum obtusidens* Schiller, and APA showed no detectable correlation with PO_4-P or DOP concentrations. These conclusions indicated that the stimulatory effect of P-stress on APA in coastal waters can be variable.

At the molecular level, microbial adaptation to P stress involves comprehensive physiological restructuring, including regulation of PO_4-P acquisition systems, extracellular enzyme synthesis, protein turnover, lipid metabolism, and adjustments to photosynthetic and respiratory pathways (Feng et al., 2015). The genetic basis of the diversity in AP responses is particularly relevant, as there are three distinct AP types (PhoAEC, PhoX, and PhoD) showing limited sequence homology yet performing similar ecological functions (Luo et al., 2009; Lin et al., 2015). Molecular adaptations

https://doi.org/10.5194/egusphere-2025-4047
Preprint. Discussion started: 19 September 2025

provide a critical insight into microbial strategies to cope with P limitation.

2. Materials and methods

2.1 Study area

Laizhou Bay (LZB), a typical semi-enclosed bay, is situated south of the Bohai Sea and north of the Shandong Peninsula (Figure 1), with an area of ca. 7,000 km², a coastline of 320 km, depth of less than 10 m, and water half-exchange time of 55 days (Wu et al., 2023). Water quality in LZB has deteriorated due to high land-based riverine inputs, e.g., from the Yellow River (YR), and Xiaoqing River (XQR), as well as from mariculture discharges. Since 1980, the dissolved inorganic nitrogen (DIN) concentration has increased from 3 to 25 $\mu mol \cdot L^{-1}$, and the ratio of DIN:PO_4-P ratio increased from 5:1 to 110:1 (Xin et al., 2019). Thus, the increase in N, coupled with P limitation have adversely affected the ecosystem in this region (Song et al., 2017).

2.2 Land and sea synchronous surveys

To investigate the distribution of APA in the LZB, four land-sea synchronous surveys were conducted on May 10–12, 2019 (spring), August 18–21, 2019 (summer), November 2–14, 2021 (autumn), and March 22–27, 2021 (winter). The land-sea synchronous survey stations covered the entire LZB and the adjacent waters of the Yellow River Estuary (YRE) (Figure 1). Monitoring stations were located at the mouths of ten rivers, including YR and XQR (Figure 1). The monitored pollutant load accounted for > 95% of the total discharge load in the LZB's basin (Li et al., 2022).

https://doi.org/10.5194/egusphere-2025-4047
Preprint. Discussion started: 19 September 2025

The August 2019 survey occurred after the landfall of the strong typhoon "Likima" in Shandong. From late August to October 2021, the middle and lower reaches of the YR experienced a historically rare autumn flood, and the November 2021 survey took place after this flood. Samples were collected in the river and sea areas quasi-synchronously.

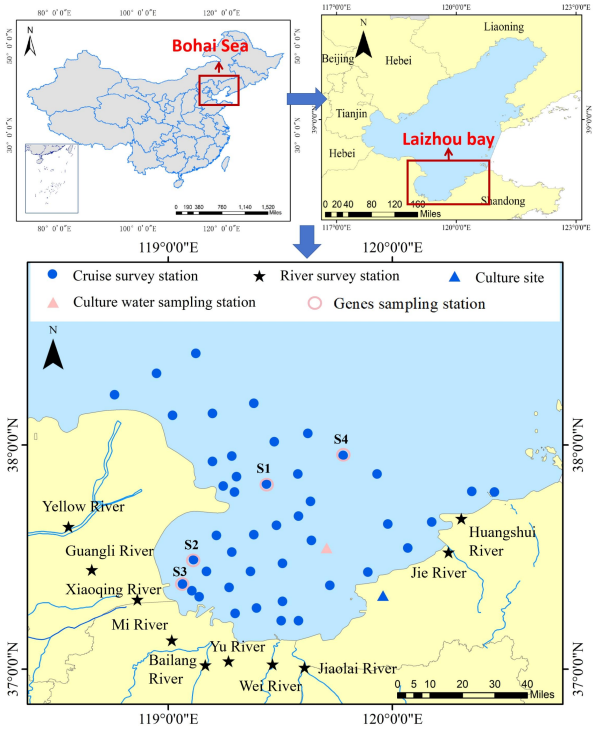

Figure 1. Synchronous sampling/survey stations in Laizhou Bay (LZB) and at river mouths around LZB.

2.3. Field enclosure experiments

An enclosure experiment was conducted from July 23 to August 21, 2021to explore the effects of phosphate concentration and DIN:PO_4-P ratio on APA secretion.

https://doi.org/10.5194/egusphere-2025-4047
Preprint. Discussion started: 19 September 2025

Two enclosed ecosystems were designed. Water samples were collected at a representative station (119.71 °E, 37.54 °N) at the mouth of LZB on July 23, 2021 (Figure 1). Seawater samples were siphoned into containment bags on the shore. Incubation experiments were carried out in the nearshore sea area (120.00 °E, 37.36 °N) for 29 days (Figure 1). The initial seawater nutrient environment with a DIN:PO_4-P ratio of 55 (Table S1) was maintained in the control group (CG). In the treatment group (TG) the DIN:PO_4-P seawater ratio was adjusted to 28 by adding $NaNO_3$ and KH_2PO_4 (Tables S1 & S2). In parallel, culture water samples were collected 17 times at fixed intervals.

2.4 Sample analysis

2.4.1. Nutrients

Nutrient samples were filtered through acetate membranes (0.45 μm pore size) and stored at -20 °C until analysis. After thawing, nutrients were measured using an automatic nutrient analyzer (SEAL-AA3, Germany). The analyzed parameters included: DIN (sum of ammonium, NH_4-N [detection limit 0.02 μM, relative standard deviation (RSD) < 2%], nitrate, NO_3-N [0.02 μM, RSD < 2%], and nitrite, NO_2-N [0.01 μM, RSD < 3%]), PO_4-P [0.01 μM, RSD < 2%], dissolved silica, DSi [0.05 μM, RSD < 3%]), total dissolved nitrogen, TDN [0.05 μM, RSD < 3%]), total dissolved phosphorus (TDP [0.02 μM, RSD < 3%]), and particulate nutrients (PN [0.1 μM, RSD < 5%]; particulate phosphorus, PP [0.05 μM, RSD < 5%]) (Murphy and Riley, 1962). TDN, TDP, and particulate nutrient concentrations were measured after the filtrates

https://doi.org/10.5194/egusphere-2025-4047
Preprint. Discussion started: 19 September 2025

and filter membranes were oxidized by persulfate at 121 °C for 30 min (Armstrong et al., 1966). Dissolved organic N and P (DON [≈0.1 μM, RSD 5-10%]; DOP [≈0.05 μM, RSD 5-10%]) were calculated as the difference between TDN/TDP and DIN/PO_4-P. respectively.

2.4.2. Chlorophyll *a*, bacterial abundance, and phytoplankton community structure

Chlorophyll *a* (Chl *a*) was extracted using 90% acetone for 24 h in the dark at 4 °C and centrifuged for 10 min at 4,000 rpm; Chl *a* concentration was measured using a fluorometer (Turner Designs-Trilogy, USA) with a detection limit of 0.025 $\mu g \cdot L^{-1}$, following methods of Parsons et al. (1984) within one month of sampling after storage of filters at -20ºC. Samples for determination of bacterial abundance were stained with SYBR Green I fluorescent dye for 20 min and measured using a BD FACSCalibur flow cytometer (BD, USA) (Marie et al., 1997). Phytoplankton community structure was determined using an inverted microscope at 400× magnification.

2.4.3. Alkaline phosphatase activity and kinetics

The fluorometric method using 4-methylumbelliferyl phosphate (MUF-P) as the substrate was employed on unfiltered (APA_{total}) and two pre-filtered (through 3 μm or 0.22 μm filters, Millipore) seawater samples. This fractionation approach allows distinguishing phosphatase activity from different microbial compartments: APA_{phy} was represented by the difference between unfiltered water samples and 3 μm-filtered water samples (mainly microalgal-associated), APA_{bac} by the difference between 3

https://doi.org/10.5194/egusphere-2025-4047
Preprint. Discussion started: 19 September 2025

μm- and 0.22 μm-filtered water samples (bacterial-associated), and APA_{free} by the activity in the 0.22 μm filtrate (extracellular enzymes), thus providing complementary information on P acquisition strategies across microbial size classes (Hoppe, 1983; Labry et al., 2005). After fixation, samples were cryopreserved at -20 °C until analysis. The fluorescence intensity of the samples was measured using a fluorescence photometer (F4700, Japan; excitation wavelength, Ex = 365 nm, emission wavelength, Em = 445 nm) immediately after thawing. Enzyme kinetic parameters V_{max} and K_m were calculated using non-linear least squares regression fitted to the Michaelis–Menten equation (Brooks, 1992). The relationship between APA and substrate concentration followed the Michaelis–Menten equation:

$$V = \frac{V_{max}S}{K_m+S} \quad (1)$$

where V represents the rate of enzymatic substrate hydrolysis (in nmol L^{-1} h^{-1}), and S the substrate concentration (in nmol L^{-1}). V_{max} represents the maximum hydrolysis rate and K_m represents the half- saturation constant, i.e., the substrate concentration at $V = \frac{1}{2}V_{max}$, (in nmol · L^{-1}).

2.4.4. Functional genomics

The DNA of the samples was extracted and characterized to investigate the microbial P metabolism pathway. The E.Z.N.A.® Soil DNA Kit (Omega Bio-tek, U.S.) was used for DNA extraction. The concentration, purity, and integrity of DNA were assessed using TBS-380, Nanodrop2000, and 1% agarose gel electrophoresis, respectively (Mäki et al., 2017). DNA fragments were segmented using a Covaris

https://doi.org/10.5194/egusphere-2025-4047
Preprint. Discussion started: 19 September 2025

M220 sonicator (Gene Company, China); fragments ca. 400 bp were screened and paired-end libraries were constructed using the NEXTFLEX Rapid DNASeq (Bioo Scientific, U.S.) library building kit. Metagenomic sequencing was performed on the Illumina NovaSeq (Illumina, U.S.) sequencing platform following bridge PCR amplification. Amino acid sequences were compared with the Kyoto Encyclopedia of Genes and Genomes (KEGG) gene database (http://www.genome.jp/kegg/) using BLASTP to obtain corresponding KEGG function information for the genes. The sum of gene abundances corresponding to Kegg Orthology (KO), Pathway, Enzyme Commission (EC) number, and Module, was used to calculate the abundances of corresponding functional categories.

2.5 Statistical analysis

Using Origin software (version 2024), the non-parametric Spearman correlation test (two-sided) was conducted to create a heat map of the correlation between APA and environmental parameters. The PO_4-P threshold was determined using a segmented regression approach. Spearman's correlation test (two-sided) was used to assess the significance of differences between two groups of data. Linear regression analysis was applied to determine whether the data were linearly correlated.

3. Results

3.1. LZB terrigenous nutrient inputs

During seasonal investigation of the rivers emptying into LZB, the average

https://doi.org/10.5194/egusphere-2025-4047
Preprint. Discussion started: 19 September 2025

annual DIN:PO_4-P ratio of riverine loads into LZB was 39:1, with a maximum of 125:1 (summer in the Jiaolai River) and a minimum of 2:1 (spring in the Bailang River) (Figure 2). The average annual total nitrogen to total phosphorus ratio (TN:TP) was 90:1, with a maximum of 263:1 (autumn in the Bailang River) and a minimum of 16:1 (spring in the Guangli River) (Figure 2). The DIN:PO_4-P ratio of riverine loads was maximal (at 70:1) in winter (Figure 2). For the P components of riverine loads, PP accounted for the highest percent contribution, with an average of 0.53 ± 0.07% (mean ± SD, standard deviation), while DOP and PO_4-P accounted for 0.27 ± 0.17% and 0.21 ± 0.16%, respectively (Figure 2). Regarding nitrogen components, DON accounted for the highest percent contribution, with an average of 0.52 ± 0.17%, and DIN and PN accounted for 0.39 ± 0.19% and 0.09 ± 0.09%, respectively (Figure 2).

https://doi.org/10.5194/egusphere-2025-4047
Preprint. Discussion started: 19 September 2025

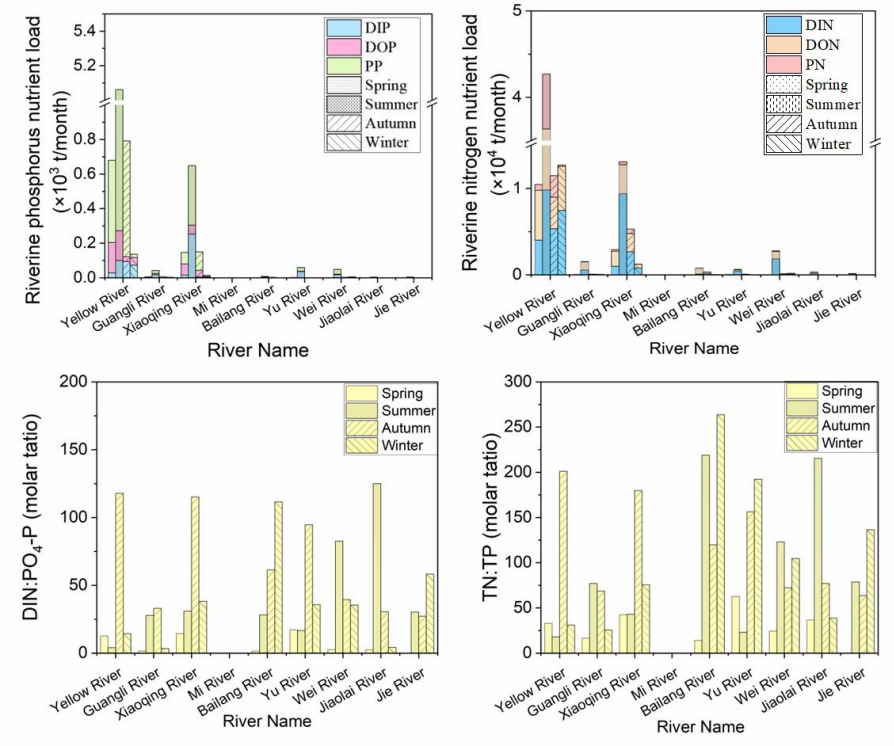

209 **Figure 2.** Seasonal phosphorus (P) and nitrogen (N) load and nutrient ratios of
210 various rivers discharging into Laizhou Bay. The Spring, summer, autumn, and winter
211 surveys were conducted in May 2019, August 2019, November 2021, and March 2021,
212 respectively. DIN and DON: dissolved inorganic and organic N, respectively; PN and
213 TN: particulate and total N, respectively.

214 3.2. Bulk parameters in LZB

215 3.2.1 Seawater temperature and salinity

216 The seawater surface layer temperature of LZB exhibited significant seasonal
217 variation ($P < 0.05$), decreasing from summer to spring, autumn, and winter, with

https://doi.org/10.5194/egusphere-2025-4047
Preprint. Discussion started: 19 September 2025

mean values of 26.2 ± 1.2 °C, 16.8 ± 2.3 °C, 12.9 ± 3.6 °C, and 6.7 ± 1.8 °C, respectively (Figure S1). The salinity of LZB showed limited seasonal variation, although it was higher in spring (27.4 ± 4.9) and winter (27.6 ± 4.5) than in summer (26.1 ± 7.1) and autumn (22.7 ± 3.6) (Figure S1).

3.2.2. Nutrients and chlorophyll *a*

During our seasonal field investigation, the average PO_4-P concentration in LZB in spring, summer, autumn and winter was 0.13 ± 0.01, 0.32 ± 0.03, 0.06 ± 0.14, 0.08 ± 0.1 $\mu mol \cdot L^{-1}$, respectively (Figure 1). In LZB PO_4-P gradually decreased with increasing distance from the shore (Figure 1). Average TP concentrations were 1.35 ± 0.26, 0.97 ± 1.42, 0.64 ± 0.42, and 0.49 ± 0.34 $\mu mol \cdot L^{-1}$ in spring, summer, autumn, and winter, respectively. The percent contributions of PO_4-P, DOP, and PP in TP were 7%, 70%, and 24% in spring; 33%, 16%, and 51% in summer; 11%, 38%, and 51% in autumn; and 24%, 14%, and 62% in winter, respectively (Figure S2). The average DIN:PO_4-P ratios of the seawater surface layer across the four seasons were 711.5 ± 423.1, 452.9 ± 500.2, 1083.6 ± 1043.7, and 363.7 ± 308.5, respectively, and thus much higher, by one or two orders of magnitude, than the 16:1 Redfield ratio (Figure S3).

The average Chl *a* concentration ± SD in spring, summer, autumn, and winter was 1.20 ± 0.98, 6.82 ± 6.14, 5.56 ± 6.28, and 6.30 ±5.99 $\mu g \cdot L^{-1}$, respectively. The ranges were 0.4 to 4.3, 0.95 to 22.10, 0.18 to 27.49, and 0.37 to 24.94 $\mu g \cdot L^{-1}$, respectively. The area characterized by relatively high Chl *a* values was mainly

https://doi.org/10.5194/egusphere-2025-4047
Preprint. Discussion started: 19 September 2025

239 distributed in the adjacent sea area of the Xiaoqing River and Yellow River estuaries
240 (Figure 3).

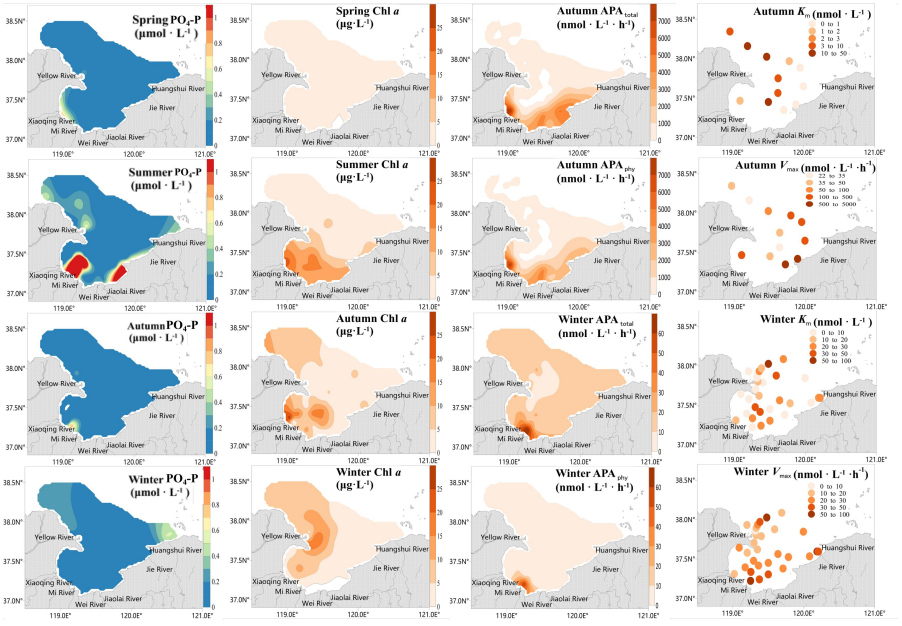

241 **Figure 3.** Planar distribution of dissolved inorganic phosphorus (PO_4-P) (μmol·L^{-1})
242 and chlorophyll *a* (Chl *a*) concentrations (in μg·L^{-1}), total and phytoplankton-derived
243 alkaline phosphatase activity (APA_{total} and APA_{phy}, respectively), (nmol · L^{-1} · h^{-1}),
244 and AP enzyme kinetic parameters (V_{max}, K_m) in Laizhou Bay in May (spring) and
245 August (ummer) 2019, and November (autumn) and March (winter) 2021.

246 3.3. Alkaline phosphatase activity and kinetics in the LZB

247 The distribution of APA in LZB showed a gradual decrease from the coastline to
248 offshore waters, such that the highest values were observed in nearshore coastal
249 waters (Figure 3). The mean value of APA_{total} reached 795.8 ± 1749.8 nmol · L^{-1} · h^{-1}
250 in autumn and was thus 50x higher than in winter (Figure 3). Mean values of APA_{phy},

https://doi.org/10.5194/egusphere-2025-4047
Preprint. Discussion started: 19 September 2025

APA_{bac}, and APA_{free} in autumn were 715.1 ± 1592.6, 55.1 ± 286.2, and 25.7 ± 61.1 nmol · L^{-1} · h^{-1}, respectively, and thus 78, 12, and 17x higher, respectively, than in winter (Figure 3; Figure S5). Accordingly, in autumn APA_{phy} contributed most to APA_{total} while APA_{free} contributed the least (Figure S6), whereas in winter APA_{free} and APA_{bac} made the highest and lowest contribution, respectively (Figure S6).

The mean value of the AP kinetic parameter K_m was 8.9 ± 13.8 ×10^3 nmol·L^{-1} in autumn and was thus 3.6x lower than in winter (31.8 ± 58.8 ×10^3 nmol·L^{-1}). In contrast, the the AP kinetic parameter V_{max} averaged 754 ± 1474.7 nmol·L^{-1}·h^{-1} in autumn, i.e., was an order of magnitude higher than in winter (26.1 ± 17.1 nmol·L^{-1}·h^{-1}) (Figure 4).

Correlation analysis of field data revealed that APA_{total}, APA_{phy}, APA_{bac}, and APA_{free} showed a significant positive correlation in autumn (Figure 4). APA_{bac} and APA_{free} exhibited a significant negative correlation with the DIN:PO_4-P ratio (r = -0.50, and -0.48, $p <= 0.05$), while APA_{phy} exhibited a significant negative correlation with the DON:TDN ratio (R, relative coefficient = -0.61, $p < 0.05$). However, there was no detectable correlation between APA and PO_4-P (Figure 4).

In winter, APA_{total}, APA_{bac}, and APA_{free} were negatively correlated with PO_4-P and Chl *a*, but not with the DIN/PO_4-P ratio (Figure 4), and APA_{total} was positively correlated with APA_{phy}, APA_{bac}, and APA_{free}. Additionally, APA_{free} was positively correlated with APA_{phy} ($r = 0.93$, $p < 0.05$) and APA_{bac} ($r = 0.49$, $p < 0.05$). APA_{total}, APA_{bac}, and APA_{free} were also positively correlated with the DON/TDN ratio (r = 0.47, 0.52, and 0.55, $p < 0.05$) (Figure 4).

https://doi.org/10.5194/egusphere-2025-4047
Preprint. Discussion started: 19 September 2025

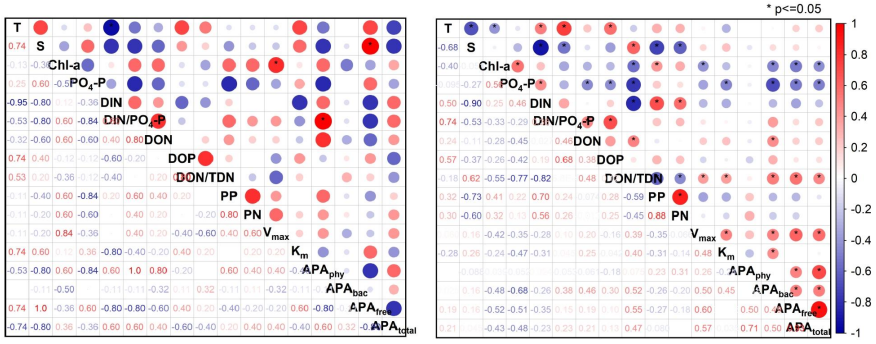

Figure 4. Heatmap of Spearman correlations between measured variables in autumn (left) and winter (right) in Laizhou Bay . Abbreviations denote: T (temperature), S (salinity), Chl *a* (chlorophyll *a*), PO_4-P (phosphate), DIN (dissolved inorganic nitrogen), DON (dissolved organic nitrogen), DOP (dissolved organic phosphorus), TDN (total dissolved nitrogen), PP (particulate phosphorus), and PN (particulate nitrogen). V_{max} and K_m represent the kinetic parameters of alkaline phosphatase. APA_{total}, APA_{phy}, APA_{bac}, and APA_{free} denote total, phytoplankton-derived, bacteria-derived, and free alkaline phosphatase activity, respectively.

3.4 Variation in APA, nutrients, and microorganisms during enclosure experiments

3.4.1 Nutrients

At the beginning of the field enclosure experiment (days 0–3, no rainfall), the control group (DIN:PO_4-P = 55) showed a high DIN:PO_4-P uptake ratio, associated with a sharp decrease in DIN concentrations and a slow decrease in PO_4-P concentrations (Figure 5a, b), resulting in a decrease in the DIN:PO_4-P ratio. In contrast, the DIN:PO_4-P uptake ratio in the TG was lower than 16:1 (Figure 5c), and

https://doi.org/10.5194/egusphere-2025-4047
Preprint. Discussion started: 19 September 2025

the DIN:PO_4-P ratio increased over time. Meanwhile, DON and DOP concentrations in the TG increased rapidly from 0 to 10 days (Figure 5d, e). Over 10-29 days, DON concentrations remained high while those of DOP slowly declined. However, in the CG, DON accumulated gradually through day 0 but DOP concentrations remained relatively constant (Figure 5d, e). Initial DON and DOP concentrations in both the CG and the TG were roughly comparable, but average DON and DOP concentrations in the TG were 1.6 and 3.6x those in the CG, respectively (Figure 5d, e).

https://doi.org/10.5194/egusphere-2025-4047
Preprint. Discussion started: 19 September 2025

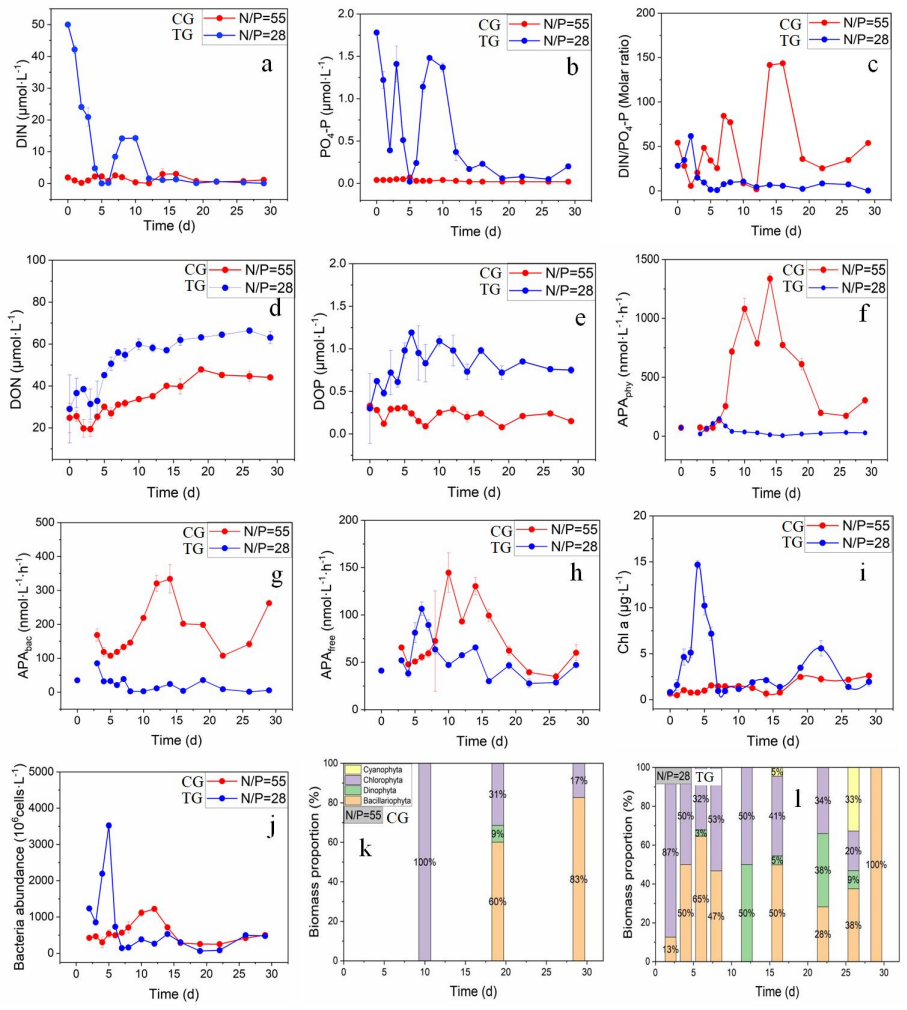

Figure 5. Dissolved nutrient concentrations, alkaline phosphatase activity (APA), chlorophyll *a* (Chl *a*) concentration, bacterial numerical abundance, and changes in percent biomass of major phytoplankton taxonomic groups over selected intervals during the 29 day-enclosure experiments N/P indicates the time-averaged nutrient ratio in the control group (TG, red line) and the treatment group (TG, blue line).

https://doi.org/10.5194/egusphere-2025-4047
Preprint. Discussion started: 19 September 2025

3.4.2. Variation in phytoplankton and bacterioplankton

Chlorophyll *a* concentrations and bacterial biomass in the TG were significantly higher than those in the CG throughout most of the experiment. Thus, the average Chl *a* and bacterial biomass in the TG were 2.9 and 1.4x greater than those in the CG, respectively (Figure 5i). In the TG, Chl *a* peaked during the early culture stage (0-6 days), reaching levels indicative of a red tide outbreak (Chl *a* ~ 15 μg · L^{-1}) (Figure 5i). Based on the analysis of phytoplankton species composition, the Chl *a* peak in the TG mainly contained diatoms (*Bacillariophyta*) and chlorophytes, and the percentage of the former also peaked during the 0-6 day-period (Figure 5l). Coincidentally, bacterial biomass also attained maximum levels during this period (Figure 5j). In the CG, Chl *a* only increased slightly (by 25%) during mid- and late culture stages, when the phytoplankton was mainly composed of diatoms and chlorophytes (Figure 5k). Bacterial biomass increased gradually during the 5 to13 day-period to attain a maximum that occurred later than that in the TG (Figure 5j).

3.3.3 Alkaline phosphatase activity

Average values of APA_{phy}, APA_{bac}, APA_{free}, and APA_{total} in the CG were 47.5, 22.6, 54.8, and 687.6 nmol·L^{-1}·h^{-1}, thus 9.3, 7.7, 1.3, and 5.6x higher, respectively, than those in the TG. In the CG, peak values of APA_{phy}, APA_{bac}, APA_{free}, and APA_{total} were 1335.8, 333.9, 144.6, and 1800.0 nmol·L^{-1}·h^{-1}, respectively, and appeared on days 10 to 16. In the TG, APA_{phy}, APA_{bac}, APA_{free}, and APA_{total} peak values were 147.38, 85.00, 106.50, and 274.75 nmol·L^{-1}·h^{-1}, appearing on days 3-6. The APA maximum in the

https://doi.org/10.5194/egusphere-2025-4047
Preprint. Discussion started: 19 September 2025

CG was mainly contributed by APA_{phy} (77%), while that in the TG was mainly contributed by APA_{phy} (50%), and APA_{free} (37%). Folowing the APA peak, Chl *a* followed an increasing trend in both CG and the TG..

3.4 Regulation of APA by both PO_4-P concentration and the DIN:PO_4-P ratio

Both field and experimental data in LZB clearly showed that APA_{phy}, APA_{bac}, and APA_{free} were synthesized and secreted when PO_4-P < 0.05 μmol · L^{-1}, and AP concentrations and activity increased rapidly as PO_4-P decreased (Figure 6). The PO_4-P threshold was consistent between the field study and enclosure experiment. At the same time, when PO_4-P was lower than its concentration threshold (0.05 μmol · L^{-1}), K_m and V_{max} also increased sharply (Figure S7). There was a significant linear positive correlation ($P < 0.01$) between APA_{total} and the DIN:PO_4-P ratio during both the autumn survey and the experiment (Figure 6). During the former, this linear relationship could be further divided into two groups, such that the slope of the fitted straight line was significantly higher in the high APA group ($P < 0.01$; line read in Figure 6) relative to that of low APA group ($P < 0.01$; line black in Figure 6). However, no obvious linear relationship was found between APA and the DIN:PO_4-P ratio in winter (Figure S8).

https://doi.org/10.5194/egusphere-2025-4047
Preprint. Discussion started: 19 September 2025

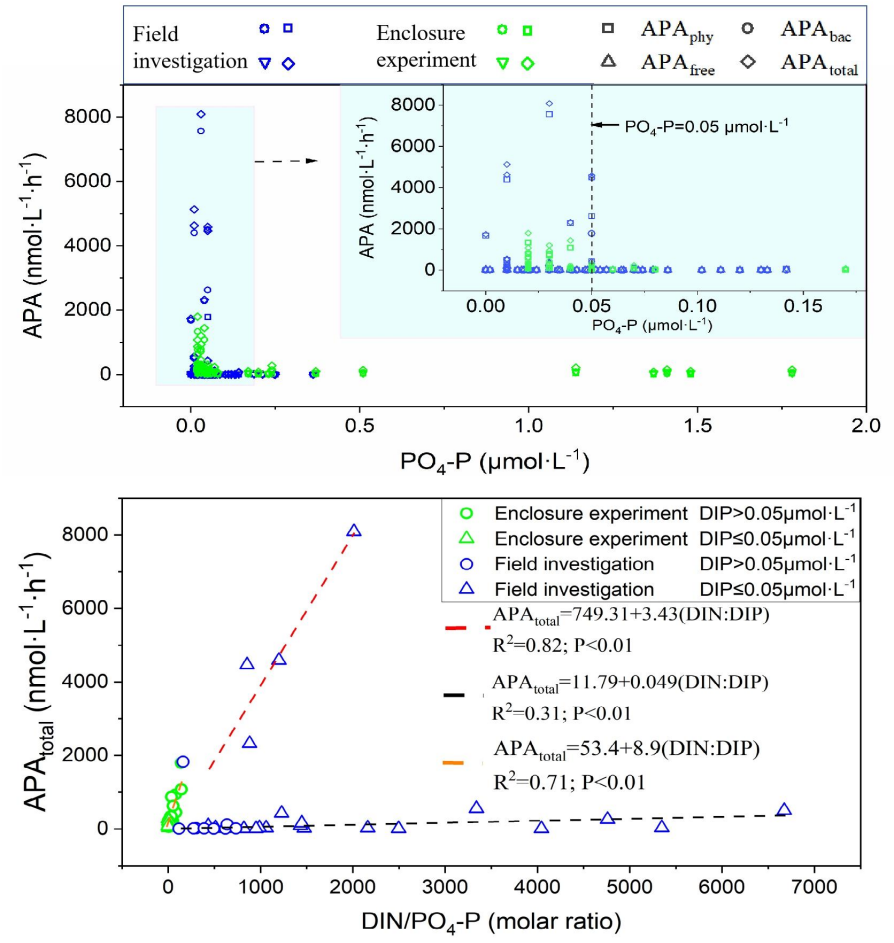

333 **Figure 6.** Phosphate (PO_4-P) concentration threshold for alkaline phosphatase activity
334 (APA) (upper graph), and fitted linear regression lines between APA_{total} and the ratio
335 of dissolved inorganic nitrogen-to-phosphate (DIN/PO_4-P) (lower graph) based on
336 data from the field study and the enclosure experiment. Fitted linear equations and the
337 coefficient of determination (R^2) are shown; APA components as in Fig. 4.

338 3.5 Functional genes for phosphorus nutrient utilization

339 During the autumn field study, the AP regulatory gene *phoD* had higher read

https://doi.org/10.5194/egusphere-2025-4047
Preprint. Discussion started: 19 September 2025

340 counts at stations with lower PO_4-P concentrations (S2_11 vs. S1_11). The former
341 also showed a significant increase in APA compared to S1_11. During the winter
342 survey, station S4_3 had relatively low PO_4-P concentrations and high APA, along
343 with high read counts for AP regulatory genes *phoD*.

344 In the CG, the PO_4-P concentration gradually decreased during the 29
345 day-experiment (Figure 5), while the AP synthesis genes (*phoD*, *phoAB*) and
346 regulatory gene (*phoP*) increased, accompanied by an increase in APA (Figure 7). In
347 the two groups with different DIN:PO_4-P ratios, the active PO_4-P concentration in the
348 CG over 29 d was lower than that in the TG over the same period (Figure 5).
349 Additionally, the read counts of *phoD*, *phoAB*, and *phoP* were higher in the CG over
350 29 d, and APA was significantly higher than in the TG over the same period ($P < 0.01$;
351 Figure 7).

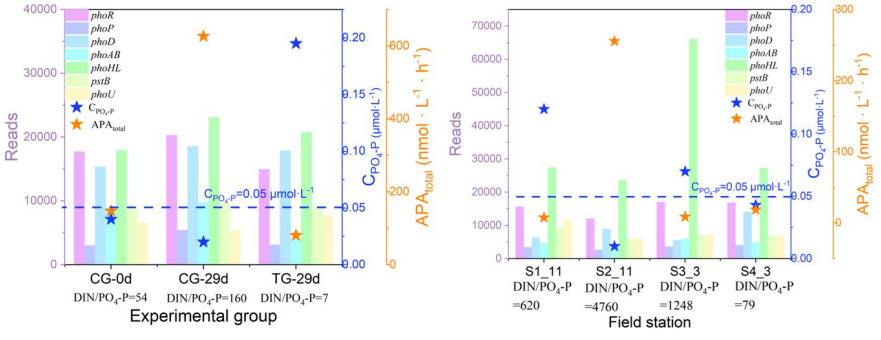

352 **Figure 7.** Changes in phosphorus (P) nutrient utilization genes and active phosphate
353 concentration ($C_{PO4\text{-}P}$) and total alkaline phosphatase activity (APA_{total}) in Laizhou
354 Bay and the experimental culture group. S1_11 and S2_11 represent data from two
355 monitoring stations in November 2021, and S3_3 and S4_3 represent data from two
356 monitoring stations in March 2021. CG-0d is the initial day for the control group,

https://doi.org/10.5194/egusphere-2025-4047
Preprint. Discussion started: 19 September 2025

while CG-29d and TG-29d represent the 29th day for the control and treatment groups, respectively (see Table S1). Genes in igure are *phoR* (phosphate regulon sensor histidine kinase), *phoP* (alkaline phosphatase synthesis response regulator), *phoD* (alkaline phosphatase D), *phoAB* (alkaline phosphatase), *phoHL* (phosphate starvation-inducible protein and related proteins), *phoB* (phosphate transport system ATP-binding protein), and *phoU* (phosphate transport system protein). Dashed horizontal lines indicate the threshold PO_4 concentration.

4. Discussion

4.1. Phosphorus limitation driven by the anthropogenic nitrogen pump in Laizhou Bay

The nutrient regime of LZB has changed markedly due to anthropogenic perturbations over the past six decades. It has shifted from a N-limited oligotrophic state before the 1990s to a potentially P-limited eutrophic state (Xin et al., 2019). Phosphorus limitation in LZB may be influenced by both anthropogenic inputs and shifts in biogeochemical processes. From the 1980s to 2020s, the DIN/PO_4-P ratio sharply increased from 200:1 to ca. 1600:1 (Xin et al., 20 19), mainly due to the effects of the YR which contributes the largest river discharge in the LZB. Our study also showed that the average N and P flux ratio of the main rivers discharging into LZB is ca. 5.6x higher than the Redfield ratio (Figure 2). The high values of the DIN:PO_4-P ratio in LZB were distributed in the nearshore area and gradually decreased moving offshore, suggesting that the terrigenous nutrient input may significantly influence the spatial distribution of the DIN:PO_4-P ratio in LZB. (Figure

https://doi.org/10.5194/egusphere-2025-4047
Preprint. Discussion started: 19 September 2025

S3). The pronounced increase in the N:P ratio of riverine nutrient loads is driven by anthropogenic activities, especially the heavy application of N fertilizer, and industrial and domestic P restrictions (Wang et al., 2019; Liang et al., 2023). Atmospheric deposition contributes ca. 30% to 50% of the total DIN of LZB (Shou et al., 2018), and only about 10 % of total phosphate (Zhang et al., 2024), leading to an N:P ratio far exceeding the 16:1 Redfield ratio (Chen et al., 2021; Zhang et al., 2024). Thus, the imbalanced input of N and P from both terrigenous and atmospheric deposition is the critical factor aggravating the N/P ratio of LZB.

The increasing DIN concentration in coastal waters, driven by anthropogenic N inputs, promotes phytoplankton growth, leading to elevated Chl *a* levels in these waters (Figure 3). Prior studies demonstrate that phytoplankton nutrient uptake under such conditions does not adhere to the classical 16:1 Redfield ratio but rather exhibits higher DIN:PO_4-P uptake ratios (Fransner et al., 2018; Macias et al., 2019). This pattern is also observed in our study where phytoplankton culture groups with high DIN:PO_4-P ratios showed correspondingly high nutrient absorption ratios (Figure 5). Under high DIN:PO_4-P ratio conditions, phytoplankton upregulate high-affinity phosphate transport systems (e.g., pstSCAB), whose Km value (Michaelis-Menten constant, reflecting the affinity of the transport system for phosphate, with lower Km indicating higher affinity) can be as low as 0.1 $\mu mol \cdot L^{-1}$ (Dyhrman & Haley, 2006). This enables efficient dissolved phosphate uptake even under extremely low P concentrations (<1 $\mu mol \cdot L^{-1}$). When P is sufficient, delayed negative feedback in the PhoB/PhoR two-component system allows continuous P uptake, with rapid

https://doi.org/10.5194/egusphere-2025-4047
Preprint. Discussion started: 19 September 2025

conversion to storage forms such as polyphosphate (polyP) (Martin et al., 2014). Concurrently, phytoplankton secrete AP to mineralize DOP, further enhancing P acquisition (Lin et al., 2016). This highly efficient P competition strategy not only exacerbates P limitation for non-storing species but also widens the range of the N:P ratio of residual dissolved inorganic nutrients due to their high N:P uptake demands (Fransner et al., 2018), creating a positive feedback loop that ultimately favors the dominance of P-storing species (Klausmeier et al., 2004).

Therefore, rather than improving the DIN:PO_4-P imbalance, biological adaptations to terrestrial high DIN:PO_4-P inputs appear to amplify and perpetuate elevated DIN:PO_4-P conditions in coastal ecosystems. This creates an ecological "trap" where the ecosystem becomes increasingly dominated by high DIN:PO_4-P-adapted species that reinforce the imbalance through their nutrient acquisition and storage strategies. Management strategies should therefore focus on reducing N:P ratios at the source rather than relying on biological compensation in the coastal zone.

4.2. AP regulation by PO_4-P concentration and the DIN:PO_4-P ratio

APA is regulated by multiple environmental factors, such as PO_4-P concentration, the DIN:PO_4-P ratio and temperature. The PO_4-P threshold (0.05 μmol·L^{-1}) identified in this study aligns with reported values from both coastal and open-ocean waters, including the semi-enclosed Bohai and Yellow Seas (Jin et al., 2024), the Sargasso Sea (Lomas et al., 2010), the eastern subtropical Atlantic (Mahaffey et al.,

https://doi.org/10.5194/egusphere-2025-4047
Preprint. Discussion started: 19 September 2025

2014), and the subtropical Pacific (Suzumura et al., 2012) (Figure 1). In the present study, both data from field surveys and the enclosure experiment confirmed this concentration threshold, with the former demonstrating a significant increase in APA and substrate affinity below this concentration. When PO_4-P concentrations fell below the threshold in autumn, a strong positive APA-DIN:PO_4-P ratio correlation was found ($P < 0.01$), consistent with observations in the Bohai Sea (Jin et al., 2024) and NW Mediterranean (Bogé et al., 2017). In winter, however, this relationship was undetectable in LZB. Furthermore, genetic analysis showed no significant AP gene upregulation at high DIN:PO_4-P ratios when PO_4-P remained above the identified threshold (station S3_3, Figure 7), confirming that sub-threshold PO_4-P concentrations are essential for APA induction. Below this threshold, APA increases proportionately with increasing DIN:PO_4-P ratios.

The phenomenon of APA surge in coastal phytoplankton reveals complex regulatory mechanisms and ecological adaptation strategies. When ambient PO_4-P concentrations fall below the 0.05-0.2 $\mu mol \cdot L^{-1}$ threshold (Dyhrman et al., 2007), phytoplankton activate the *pho* regulon operon (a gene cluster containing the pstSCAB phosphate transport system and phoA/phoX alkaline phosphatase genes) through the *PhoB/PhoR* two-component system (a P-sensing system consisting of histidine kinase *PhoR* and the response regulator PhoB) (Lin et al., 2016). Notably, our findings demonstrate a significant positive correlation between APA and the DIN:PO_4-P ratio when PO_4-P concentrations fall below the threshold. This result may stem from the following fundamental mechanisms: (1) High DIN:PO_4-P conditions

https://doi.org/10.5194/egusphere-2025-4047
Preprint. Discussion started: 19 September 2025

induce an enhanced capacity for P acquisition to maintain elemental stoichiometric balance, manifested as increased APA with rising DIN:PO_4-P ratios; (2) Elevated DIN:PO_4-P ratios may indirectly modulate APA through N-sensitive regulators (e.g., PII protein) in the pho signaling pathway (Ustick et al., 2021).

It is noteworthy that prior studies have found that under the same N:P ratio and active phosphate concentration, phytoplankton APA in DON-enriched cultures was significantly higher than that in cultures without DON (Fitzsimons et al., 2020). Our winter survey data revealed a significant positive correlation between DON and APA_{bac} (Figure 4), similar to findings of APA_{phyto} and DON concentration (Ou et al., 2024), indicating that not only PO_4-P but also nutrient composition and ratios, can affect APA. Regulation of APA by DON may potentially operate through specific DON components or their degradation products influencing P metabolic pathways, or through DON serving as an alternative N source that stimulates phytoplankton growth and P demand (Ma et al., 2018; Forchhammer et al., 2022).

4.3. Conceptual framework of anthropogenic N pump-driven APA regulatory cascades

Human activities have significantly altered coastal nutrient dynamics via multi-level ecological feedback mechanisms that regulate APA activity patterns (Figure 8). The "anthropogenic N pump" driven by riverine discharge and atmospheric deposition (Jin et al., 2023) has induced a disproportionate increase in DIN inputs, leading to relative PO_4-P depletion and elevated DIN:PO_4-P ratios (Figures 2 and 3). This nutrient imbalance triggers phytoplankton adaptive responses,

https://doi.org/10.5194/egusphere-2025-4047
Preprint. Discussion started: 19 September 2025

i.e., when PO_4-P concentrations fall below the identified threshold, the *pho* regulon and other APA-related gene clusters are activated (Figure 7), while the combined effects of high DIN:PO_4-P ratios and P limitation significantly enhance APA expression and DOP mineralization capacity (Figure 6). These biochemical responses initiate ecological cascades that favor phytoplankton with high APA activity and superior DOP utilization capabilities (Figure S3; Hackett et al., 2005; Nicholson et al., 2006; Ivancic et al., 2016; Ou et al., 2024). Variation in seasonal temperature regulates this process both through direct suppression of APA activity (via reduced enzymatic kinetics and microbial metabolism) and indirect modulation of community composition (reflecting thermal niche differentiation among phytoplankton groups) (Toseland et al., 2013; Thomas et al., 2017).

The above system ultimately establishes a positive feedback loop: APA-mediated DOP utilization increases phytoplankton biomass (as reflected in elevated Chl *a*), which accelerates PO_4-P depletion and exacerbates the DIN:PO_4-P imbalance, thereby continuously selecting for APA-enhanced genotypes. This conceptual framework demonstrates how anthropogenic alteration of DIN:PO_4-P stoichiometry triggers cross-scale responses from molecular to ecosystem levels, creating self-reinforcing ecological restructuring.

https://doi.org/10.5194/egusphere-2025-4047
Preprint. Discussion started: 19 September 2025

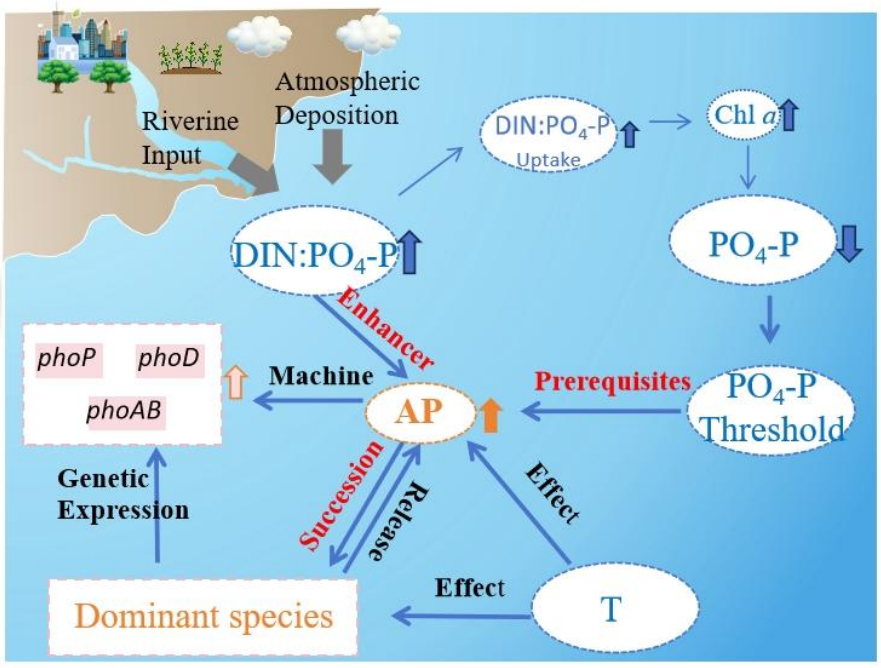

482 **Figure 8.** Conceptual framework of anthropogenic, nitrogen pump-driven regulatory
483 cascades of alkaline phosphate activity (APA) in Laizhou Bay. Abbreviations as in
484 previous figures.

485 **5. Conclusions**

486 This study confirmed the existence of a PO_4-P threshold for APA activation in
487 both phytoplankton and bacteria in LZB, China, using a combination of field studies
488 and enclosed experimentation. The thresholds for APA surges in phytoplankton and
489 bacteria were comparable, with no significant differences observed between them.
490 Results of the relationship between enzyme kinetic parameters and environmental
491 parameters further validate the existence of a PO_4-P threshold. When PO_4-P levels fell
492 below this threshold, AP-related gene expression increased at survey stations and in

https://doi.org/10.5194/egusphere-2025-4047
Preprint. Discussion started: 19 September 2025

493 culture experiments resulting in high APA. We conclude that in LZB, APA was
494 primarily regulated by PO_4-P concentration, the DIN:PO_4-P ratio, and phytoplankton
495 biomass. Typically, a linear positive correlation was found between APA and the
496 DIN:PO_4-P ratio under low P stress. Most importantly, this study refines the
497 conceptual theory of AP's role in the P cycle under the influence of anthropogenic
498 activities: PO_4-P concentrations exceeding the threshold value are a prerequisite for
499 observed APA surges, and the DIN:PO_4-P ratio is the primary environmental factor
500 driving the increase in APA when PO_4-P concentration is below the identified
501 threshold.

502 **CrediT authorship contribution statement**

503 **YY**: writing of the draft, methodology, data analysis and curation. **XD**: methodology,
504 data analysis and curation; **SL**: methodology, provision of resources for the study,
505 review and editing of the manuscript, research supervision; **MZ**, **SL**, **HL**, **GZ**, **HM**,
506 and **XH**: data curation; **XW**: research supervision.

507 **Declaration of competing interest**

508 The authors declare no conflict of interest.

509 **Acknowledgments**

510 This research was funded by the National Key Research and Development Project of
511 China (No. 2018YFC1407602), and the Fundamental Research Founds for the Central
512 Universities (grant number 202464007, 202472007).

https://doi.org/10.5194/egusphere-2025-4047
Preprint. Discussion started: 19 September 2025

References

Armstrong, F. A. J., P. M. Williams, and J. D. H. Strickland. 1966. Photo-oxidation of organic matter in sea water by ultra-violet radiation, analytical and other applications. Nature 211:481–483.

Bogé, G., Lespilette, M., Jamet, D. and Jamet, J.L., 2017. Role of DOP on the alkaline phosphatase activity of size fractionated plankton in coastal waters in the NW Mediterranean Sea (Toulon Bay, France). Marine Pollution Bulletin. 117, 264-273, DOI10.1016/j.marpolbul.2016.11.037.

Brooks, S.P.J., 1992. A simple computer program with statistical tests for the analysis of enzyme kinetics. Biotechnology 13, 906 – 911.

Browning, T.J., Achterberg, E.P., Yong, J.C., Rapp, I., Utermann, C., Engel, A. and Moore, C.M., 2017. Iron limitation of microbial phosphorus acquisition in the tropical North Atlantic. Nature Communications. 8, 7, DOI10.1038/ncomms15465.

Castle, S.C., Morrison, C.D., Barger, N.N., 2011. Extraction of chlorophyll a from biological soil crusts: a comparison of solvents for spectrophotometric determination. Soil Biol. Biochem. 43 (4), 853–856, DOI10.1016/j.soilbio.2010.11.025.

Chen, H.Y., Huang, L.M., Ho, T.Y., Chiang, K.P. and Chou, W.C., 2021. A study of the nitrogen and phosphorus imbalance in East Asia based on the distribution patterns of and stoichiometric variation in global atmospheric nitrogen and phosphorus. Atmospheric Environment. 266, 12,

https://doi.org/10.5194/egusphere-2025-4047
Preprint. Discussion started: 19 September 2025

DOI10.1016/j.atmosenv.2021.118691.

Duhamel, S., Björkman, K.M., Van Wambeke, F., Moutin, T. and Karl, D.M., 2011. Characterization of alkaline phosphatase activity in the North and South Pacific Subtropical Gyres: Implications for phosphorus cycling. Limnology and Oceanography. 56, 1244-1254, DOI10.4319/lo.2011.56.4.1244.

Dyhrman, S.T. and Ruttenberg, K.C., 2006. Presence and regulation of alkaline phosphatase activity in eukaryotic phytoplankton from the coastal ocean: Implications for dissolved organic phosphorus remineralization. Limnology and Oceanography. 51, 1381-1390, DOI10.4319/lo.2006.51.3.1381.

Dyhrman, S.T., Chappell, P.D., Haley, S.T., Moffett, J.W., Orchard, E.D., Waterbury, J.B., Webb, E.A., 2006. Phosphonate utilization by the globally important marine diazotroph *Trichodesmium*. Nature 439, 68-71, DOI10.1038/nature04203.

Dyhrman, S.T., Haley, S.T., 2006. Phosphorus scavenging in the unicellular marine diazotroph *Crocosphaera watsonii*. Appl. Environ. Microbiol. 72, 1452-1458, DOI10.1128/AEM.72.2.1452-1458.2006.

Feng, T.Y., Yang, Z.K., Zheng, J.W., Xie, Y., Li, D.W., Murugan, S.B., Yang, W.D., Liu, J.S. and Li, H.Y., 2015. Examination of metabolic responses to phosphorus limitation via proteomic analyses in the marine diatom *Phaeodactylum tricornutum*. Scientific Reports. 5, 10, DOI10.1038/srep10373.

Fitzsimons, M.F., Probert, I., Gaillard, F. and Rees, A.P., 2020. Dissolved organic phosphorus uptake by marine phytoplankton is enhanced by the presence of dissolved organic nitrogen. Journal of Experimental Marine Biology and Ecology.

https://doi.org/10.5194/egusphere-2025-4047
Preprint. Discussion started: 19 September 2025

530, 9, DOI10.1016/j.jembe.2020.151434.

Fonseca-Batista, D., Dehairs, F., Riou, V., Fripiat, F., Elskens, M., Deman, F., Brion, N., Quéroué, F., Bode, M., Auel, H., 2017. Nitrogen fixation in the eastern Atlantic reaches similar levels in the Southern and Northern Hemisphere. J. Geophys. Res.-Oceans 122, 587-601, DOI10.1002/2016JC012335.

Forchhammer, K., Selim, K.A., Huergo, L.F., 2022. New views on PII signaling: from nitrogen sensing to global metabolic control. Trends Microbiol. 30, 722-735, DOI10.1016/j.tim.2021.12.014.

Fransner, F., Gustafsson, E., Tedesco, L., Vichi, M., Hordoir, R., Roquet, F., Spilling, K., Kuznetsov, I., Eilola, K., Mörth, C.M., Humborg, C. and Nycander, J., 2018. Non-Redfieldian Dynamics Explain Seasonal pCO_2 Drawdown in the Gulf of Bothnia. Journal of Geophysical Research-Oceans. 123, 166-188, DOI10.1002/2017JC013019.

Hackett, J.D., Scheetz, T.E., Yoon, H.S., Soares, M.B., Bonaldo, M.F., Casavant, T.L. and Bhattacharya, D., 2005. Insights into a dinoflagellate genome through expressed sequence tag analysis. Bmc Genomics. 6, 13, DOI10.1186/1471-2164-6-80.

Hoppe, H.G., 1983. Significance of exoenzymatic activities in the ecology of brackish water: measurements by means of methylumbelliferyl-substrates. Marine Ecology Progress Series. 11, 299 – 308.

Ivancic, I., Kraus, R., Najdek, M. and Cozzi, S., 2021. Ecological Importance of Alkaline Phosphatase Activity in Changing Marine Environmental Conditions.

https://doi.org/10.5194/egusphere-2025-4047
Preprint. Discussion started: 19 September 2025

Water. 13, 25, DOI10.3390/w13192750.

Ivancic, I., Pfannkuchen, M., Godrijan, J., Djakovac, T., Pfannkuchen, D.M., Korlevic, M., Gasparovic, B. and Najdek, M., 2016. Alkaline phosphatase activity related to phosphorus stress of microphytoplankton in different trophic conditions. Progress in Oceanography. 146, 175-186, DOI10.1016/j.pocean.2016.07.003.

Jin, H., Zhang, C., Meng, S., Wang, Q., Ding, X., Meng, L., Zhuang, Y., Yao, X., Gao, Y., Shi, F., Mock, T. and Gao, H., 2024. Atmospheric deposition and river runoff stimulate the utilization of dissolved organic phosphorus in coastal seas. Nature communications. 15, 658, DOI10.1038/s41467-024-44838-7.

Kang, W., Wang, Z.H., Liu, L. and Guo, X., 2019. Alkaline phosphatase activity in the phosphorus-limited southern Chinese coastal waters. Journal of Environmental Sciences. 86, 38-49, DOI10.1016/j.jes.2019.04.026.

Karl, D.M., 2014. Microbially Mediated Transformations of Phosphorus in the Sea: New Views of an Old Cycle, in: Carlson, C.A. and Giovannoni, S.J. Eds.), Annual Review of Marine Science, Vol 6. Annual Reviews, Palo Alto, pp. 279-337, DOI10.1146/annurev-marine-010213-135046.

Klausmeier, C.A., Litchman, E., Daufresne, T., Levin, S.A., 2004. Optimal nitrogen-to-phosphorus stoichiometry of phytoplankton. Nature 429, 171-174, DOI10.1038/nature02454.

Labry, C., Delmas, D. and Herbland, A., 2005. Phytoplankton and bacterial alkaline phosphatase activities in relation to phosphate and DOP availability within the Gironde plume waters (Bay of Biscay). Journal of Experimental Marine Biology

https://doi.org/10.5194/egusphere-2025-4047
Preprint. Discussion started: 19 September 2025

and Ecology. 318, 213-225, DOI10.1016/j.jembe.2004.12.017.

Li, H.G., Li, X.R., Xu, Z.H., Liang, S.K., Ding, Y., Song, D.H. and Guo, H., 2022. Nutrient budgets for the Bohai Sea: Implication for ratio imbalance of nitrogen to phosphorus input under intense human activities. Marine Pollution Bulletin. 179, 9, DOI10.1016/j.marpolbul.2022.113665.

Liang, W., Wang, Y., Mu, J.L., Wu, N., Wang, J.Y. and Liu, S.M., 2023. Nutrient changes in the Bohai Sea over the past two decades. Science of the Total Environment. 903, 16, DOI10.1016/j.scitotenv.2023.166696.

Lin, S.J., Litaker, R.W. and Sunda, W.G., 2016. Phosphorus physiological ecology and molecular mechanisms in marine phytoplankton. Journal of Phycology. 52, 10-36, DOI10.1111/jpy.12365.

Lin, X., Wang, L., Shi, X.G. and Lin, S.J., 2015. Rapidly diverging evolution of an atypical alkaline phosphatase ($PhoA^{aty}$) in marine phytoplankton: insights from dinoflagellate alkaline phosphatases. Frontiers in Microbiology. 6, 12, DOI10.3389/fmicb.2015.00868.

Lin, X., Zhang, H., Huang, B.Q., Lin, S.J., 2012. Alkaline phosphatase gene sequence characteristics and transcriptional regulation by phosphate limitation in *Karenia brevis* (Dinophyceae). Harmful Algae 17, 14-24, DOI10.1016/j.hal.2012.02.005.

Lomas, M.W., Burke, A.L., Lomas, D.A., Bell, D.W., Shen, C., Dyhrman, S.T. and Ammerman, J.W., 2010. Sargasso Sea phosphorus biogeochemistry: an important role for dissolved organic phosphorus (DOP). Biogeosciences. 7, 695-710, DOI10.5194/bg-7-695-2010.

https://doi.org/10.5194/egusphere-2025-4047
Preprint. Discussion started: 19 September 2025

623 Luo, H.W., Benner, R., Long, R.A. and Hu, J.J., 2009. Subcellular localization of
624 marine bacterial alkaline phosphatases. Proceedings of the National Academy of
625 Sciences of the United States of America. 106, 21219-21223,
626 DOI10.1073/pnas.0907586106.
627 Ma, S.N., Wang, H.J., Wang, H.Z., Li, Y., Liu, M., Liang, X.M., Yu, Q., Jeppesen, E.,
628 Sondergaard, M., 2018. High ammonium loading can increase alkaline
629 phosphatase activity and promote sediment phosphorus release: A two-month
630 mesocosm experiment. Water Res. 145, 388-397,
631 DOI10.1016/j.watres.2018.08.043.
632 Maavara, T., Akbarzadeh, Z. and Van Cappellen, P., 2020. Global Dam-Driven
633 Changes to Riverine N:P:Si Ratios Delivered to the Coastal Ocean. Geophysical
634 Research Letters. 47, 9, DOI10.1029/2020GL088288.
635 Macias, D., Huertas, I.E., Garcia-Gorriz, E. and Stips, A., 2019. Non-Redfieldian
636 dynamics driven by phytoplankton phosphate frugality explain nutrient and
637 chlorophyll patterns in model simulations for the Mediterranean Sea. Progress in
638 Oceanography. 173, 37-50, DOI10.1016/j.pocean.2019.02.005.
639 Mäki, A., Salmi, P., Mikkonen, A., Kremp, A. and Tiirola, M., 2017. Sample
640 Preservation, DNA or RNA Extraction and Data Analysis for High-Throughput
641 Phytoplankton Community Sequencing. Frontiers in Microbiology. 8, 13,
642 DOI10.3389/fmicb.2017.01848.
643 Marie, D., Partensky, F., Jacquet, S. and Vaulot, D., 1997. Enumeration and cell cycle
644 analysis of natural populations of marine picoplankton by flow cytometry using

https://doi.org/10.5194/egusphere-2025-4047
Preprint. Discussion started: 19 September 2025

the nucleic acid stain SYBR Green I. Applied and Environmental Microbiology. 63, 186-193, DOI10.1128/AEM.63.1.186-193.1997.

Martin, P., Van Mooy, B.A.S., Heithoff, A., Dyhrman, S.T., 2011. Phosphorus supply drives rapid turnover of membrane phospholipids in the diatom *Thalassiosira pseudonana*. Isme J. 5, 1057-1060, DOI10.1038/ismej.2010.192.

Mayers, J.J., Flynn, K.J. and Shields, R.J., 2014. Influence of the N:P supply ratio on biomass productivity and time-resolved changes in elemental and bulk biochemical composition of *Nannochloropsis* sp. Bioresource Technology. 169, 588-595., https://doi.org/10.1016/j.biortech.2014.07.048

Meseck, S.L., Alix, J.H., Wikfors, G.H. and Ward, J.E., 2009. Differences in the Soluble, Residual Phosphate Concentrations at Which Coastal Phytoplankton Species Up-regulate Alkaline-Phosphatase Expression, as Measured By Flow-Cytometric Detection of ELF-97A® Fluorescence. Estuaries and Coasts. 32, 1195-1204, DOI10.1007/s12237-009-9211-7.

Mo, Y., Ou, L.J., Lin, L.Z. and Huang, B.Q., 2020. Temporal and spatial variations of alkaline phosphatase activity related to phosphorus status of phytoplankton in the East China Sea. Science of the Total Environment. 731, 10, DOI10.1016/j.scitotenv.2020.139192.

Murphy, J., and J. P. Riley. 1962. A modified single solution method for the determination of phosphate in natural waters. Anal. Chim. Acta 27:31–36.

Nausch, M., 1998. Alkaline phosphatase activities and the relationship to inorganic phosphate in the Pomeranian bight (southern Baltic Sea). Aquat. Microb. Ecol.

https://doi.org/10.5194/egusphere-2025-4047
Preprint. Discussion started: 19 September 2025

16, 87 – 94, DOI10.3354/ame016087.

Nicholson, D., S. Dyhrman, F. Chavez, and A. Paytan. 2006. Alkaline phosphate activity in the phytoplankton communities of Monterey Bay and San Francisco Bay. Limnology and Oceanography 51: 874–883, DOI10.4319/lo.2006.51.2.0874.

Ou, L.J., Qin, X.L., Shi, X.Y., Feng, Q.L., Zhang, S.W., Lu, S.H., Qi, Y.Z., 2020. Alkaline phosphatase activities and regulation in three harmful Prorocentrum species from the coastal waters of the East China Sea. Microbial Ecology. 79, 459–471, DOI: 10.1007/s00248-019-01399-3.

Ou, L.J., Wang, Z., Ding, G.M., Han, F.X., Cen, J.Y., Dai, X.F., Li, K.Q. and Lu, S.H., 2024. Organic nutrient availability and extracellular enzyme activities influence harmful algal bloom proliferation in a coastal aquaculture area. Aquaculture. 582, 9, DOI10.1016/j.aquaculture.2023.740530.

Parsons T R, Maita Y, Lalli C M. 1984. A manual of chemical and biological methods for sea water analysis. In: Parsons T R, Takahashi M, Hargrave B, ed. Biological Oceanographic Processes. 3rd ed. New York: Pergamon Press, 173

Peñuelas, J. and Sardans, J., 2022. The global nitrogen-phosphorus imbalance. Science. 375, 266-267, DOI10.1126/science.abl4827.

Shou, W.W., Zong, H.B., Ding, P.X. and Hou, L.J., 2018. A modelling approach to assess the effects of atmospheric nitrogen deposition on the marine ecosystem in the Bohai Sea, China. Estuarine Coastal and Shelf Science. 208, 36-48, DOI10.1016/j.ecss.2018.04.025.

https://doi.org/10.5194/egusphere-2025-4047
Preprint. Discussion started: 19 September 2025

689 Song, D.B., Gao, Z.Q., Zhang, H., Xu, F.X., Zheng, X.Y., Ai, J.Q., Hu, X.K., Huang,
690 G.P. and Zhang, H.B., 2017. GIS-based health assessment of the marine
691 ecosystem in Laizhou Bay, China. Marine Pollution Bulletin. 125, 242-249,
692 DOI10.1016/j.marpolbul.2017.08.027 .
693 Suzumura, M., Hashihama, F., Yamada, N. and Kinouchi, S., 2012. Dissolved
694 phosphorus pools and alkaline phosphatase activity in the euphotic zone of the
695 western North Pacific Ocean. Frontiers in Microbiology. 3, 13,
696 DOI10.3389/fmicb.2012.00099.
697 Thomas, M.K., Aranguren-Gassis, M., Kremer, C.T., Gould, M.R., Anderson, K.,
698 Klausmeier, C.A., Litchman, E., 2017. Temperature-nutrient interactions
699 exacerbate sensitivity to warming in phytoplankton. Glob. Change Biol. 23,
700 3269-3280, DOI10.1111/gcb.13641.
701 Toseland, A., Daines, S.J., Clark, J.R., Kirkham, A., Strauss, J., Uhlig, C., Lenton,
702 T.M., Valentin, K., Pearson, G.A., Moulton, V., Mock, T., 2013. The impact of
703 temperature on marine phytoplankton resource allocation and metabolism. Nat.
704 Clim. Chang. 3, 979-984, DOI10.1038/NCLIMATE1989.
705 Ustick, L.J., Larkin, A.A., Garcia, C.A., Garcia, N.S., Brock, M.L., Lee, J.A.,
706 Wiseman, N.A., Moore, J.K., Martiny, A.C., 2021. Metagenomic analysis reveals
707 global-scale patterns of ocean nutrient limitation. Science 372, 287-+,
708 DOI10.1126/science.abe6301.
709 Van Mooy, B.A.S., Rocap, G., Fredricks, H.F., Evans, C.T. and Devol, A.H., 2006.
710 Sulfolipids dramatically decrease phosphorus demand by picocyanobacteria in

https://doi.org/10.5194/egusphere-2025-4047
Preprint. Discussion started: 19 September 2025

711 oligotrophic marine environments. Proceedings of the National Academy of
712 Sciences of the United States of America. 103, 8607-8612,
713 DOI10.1073/pnas.0600540103.
714 Wang, J.J., Yu, Z.G., Wei, Q.S. and Yao, Q.Z., 2019. Long-Term Nutrient Variations in
715 the Bohai Sea Over the Past 40 Years. Journal of Geophysical Research-Oceans.
716 124, 703-722, DOI10.1029/2018JC014765.
717 Wu, Z.C., Zhou, C.Y., Wang, P. and Fei, Z.H., 2023. Responses of tidal dynamic and
718 water exchange capacity to coastline change in the Bohai Sea, China. Frontiers in
719 Marine Science. 10, 11, DOI10.3389/fmars.2023.1118795.
720 Xin, M., Wang, B.D., Xie, L.P., Sun, X., Wei, Q.S., Mang, S.K. and Chen, K., 2019.
721 Long-term changes in nutrient regimes and their ecological effects in the Bohai
722 Sea, China. Marine Pollution Bulletin. 146, 562-573,
723 DOI10.1016/j.marpolbul.2019.07.011.
724 Yamaguchi, T., Furuya, K., Sato, M. and Takahashi, K., 2016. Phosphate release due
725 to excess alkaline phosphatase activity in *Trichodesmium erythraeum*. Plankton
726 & Benthos Research. 11, 29-36, DOI10.3800/pbr.11.29.
727 Yang, Y., Pan, J.Y., Han, B.P. and Naselli-Flores, L., 2020. The effects of absolute and
728 relative nutrient concentrations (N/P) on phytoplankton in a subtropical reservoir.
729 Ecological Indicators. 115, 9, DOI10.1016/j.ecolind.2020.106466.
730 Zhang, C., Luo, H., Huang, L.M. and Lin, S.J., 2017. Molecular mechanism of
731 glucose-6-phosphate utilization in the dinoflagellate Karenia mikimotoi. Harmful
732 Algae. 67, 74-84, DOI10.1016/j.hal.2017.06.006.

https://doi.org/10.5194/egusphere-2025-4047
Preprint. Discussion started: 19 September 2025

733 Zhang, S.F., Chen, Y., Xie, Z.X., Zhang, H., Lin, L. and Wang, D.Z., 2019.
734 Unraveling the molecular mechanism of the response to changing ambient
735 phosphorus in the dinoflagellate *Alexandrium catenella* with quantitative
736 proteomics. Journal of Proteomics. 196, 141-149,
737 DOI10.1016/j.jprot.2018.11.004.
738 Zhang, X. J., C. G. Tian, Z. Y. Sun, X. H. Yin, R. Sun, and J. Y. Wang, 2024.
739 Temporal and Spatial Distribution of DIN and PO_4-P Concentrations and Source
740 Apportionment Along the Bohai Sea of China During 2015-2022. Chinese
741 Geographical Science. 34(6): 1004-16,
742 https://doi.org/10.1007/s11769-024-1464-3.
743 Zhang, X.S., Yu, K.L., Li, M., Jiang, H., Gao, W.M., Zhao, J. and Li, K.Q., 2024.
744 Diatom-dinoflagellate succession in the Bohai Sea: The role of N/P ratios and
745 dissolved organic nitrogen components. Water Research. 251, 12,
746 DOI10.1016/j.watres.2024.121150.
747